

Safe Real-World Reinforcement Learning for Mobile Agent Obstacle Avoidance

Mario Srouji, Wei Ding, Yao-Hung Hubert Tsai, Ali Farhadi, Jian Zhang

Abstract—Collision avoidance is key for mobile robots and agents to operate safely in the real world. In this work, we present an efficient and effective collision avoidance system that combines real-world reinforcement learning (RL), search-based online trajectory planning, and automatic emergency intervention, e.g. automatic emergency braking (AEB). The goal of the RL is to learn effective search heuristics that speed up the search for collision-free trajectory and reduce the frequency of triggering automatic emergency interventions. This novel setup enables RL to learn safely and directly on mobile robots in a real-world indoor environment, minimizing actual crashes even during training. Our real-world experiments show that, when compared with several baselines, our approach enjoys a higher average speed, lower crash rate, higher goals reached rate, smaller computation overhead, and smoother overall control.

I. INTRODUCTION

Due to advances in artificial intelligence and robotics, autonomous agents have more comprehensive abilities, with applications in vacuum cleaning, video recording, companionship, security, etc. Collision avoidance is key for mobile agents that operate safely in the real world and avoid damage to the agent, surrounding environment, and humans. There are numerous approaches to collision avoidance, including search-based planning methods, trajectory optimization, learning-based methods, and emergency intervention systems. Search-based trajectory planning methods are successful at finding collision-free trajectories if given good discretization, enough computation, and ideal search heuristics, however, due to the size of the search space in real-world continuous problems, the search could be too computationally heavy to yield good enough solutions [5] [17] [28] [26] [2]. Trajectory optimization is able to solve for locally optimal trajectories for collision avoidance, however, it requires very good initialization, sophisticated cost and constraint modeling to guarantee continuity and feasibility [30] [23] [4]. Learning-based methods are promising as they are data-driven and run inference on GPU or AI accelerator to achieve the fast and fixed computation, however, it is difficult to ensure safety due to distribution shift and uncertainties, especially during training [6], [11]. Another approach is automatic emergency intervention system, e.g. automatic emergency braking (AEB), which sacrifices optimality in exchange for fast computation and low false negative rate, by bringing the agent to a complete stop reactively in an emergency [14] [10] [22].

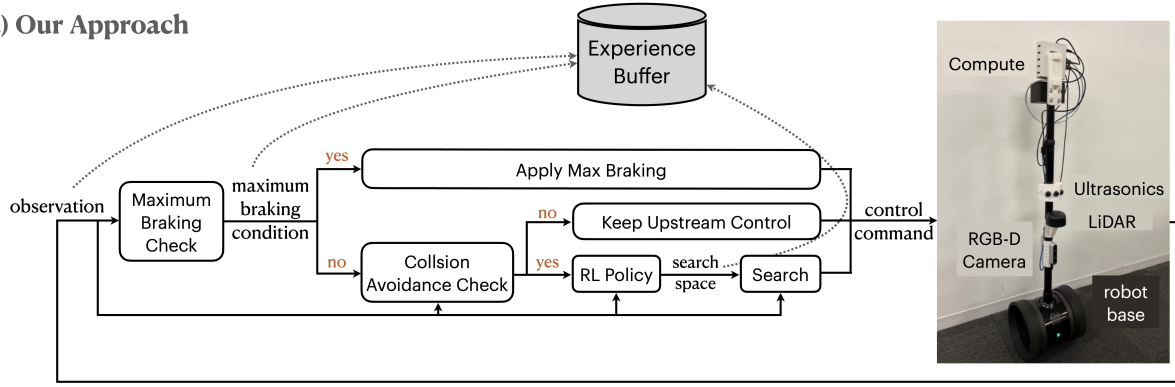
The AEB is activated when the agent has encountered an unsafe state that requires immediate takeover. Our key insight is that even though this unsafe state could be a false positive in certain situations, e.g. when the robot could avoid the

head-on collision by swerving to the side, it can be treated as a conservative signal for imminent collision. Our approach treats this conservative signal as a learning signal, i.e. we want to plan ahead by learning to avoid getting into unsafe conditions, thus reducing its frequency of activation and avoiding stop-and-go behaviors. Specifically, we leverage AEB activation as a learning signal to search corrective control commands to an agent’s upstream control (could be from human control or other upstream algorithms) when detecting potential collisions. Since we want our collision avoidance search to be efficient, we focus on restricting the search space over corrective control actions, which is important to reduce the latency of our method, especially in a dynamic environment with humans.

Our collision avoidance system takes input from lidar and ultrasonic sensor scans, wheel odometry for robot state, and the upstream control commands. We fuse the lidar and ultrasonic sensor scans to detect a diverse set of obstacles, including transparent glass, reflective surfaces, furniture, humans, etc. The RL-guided search introduces additional parameters to shrink the search window in the Dynamic Window Approach (DWA) method [5], for an efficient search over control commands that avoid AEB. We design a reward function for our RL agent with three terms to accomplish this. The first term encourages the reduction of AEB activation. The second term improves collision avoidance metrics such as average speed, smoothness, distance to obstacles, etc. Finally, the third term encourages restricting the search space over possible corrective control commands. Our method learns directly in a real-world indoor office environment by using a distributed RL training setup, leveraging the Soft Actor Critic (SAC) [8] algorithm. Multiple robots collect experience through a higher-level navigation policy, and a centralized training server collects experiences and updates the RL policy that is shared by all robots. With this novel setup, we can perform real-world RL training while minimizing actual crashes throughout the learning process, avoiding potential physical damage.

Our experiments show that, when compared to both traditional and learning-based methods, our approach demonstrates a higher average speed for the robotic agents, lower collision rate, higher goal-reaching rate, lower computational overhead, and is able to perform training directly in a real world environment with minimum actual crashes. We believe this work opens up a new approach for safer learning in the real world, and thus accelerates the development of intelligent agents.

(a) Our Approach



(b) Environments



(c) Search Comparisons

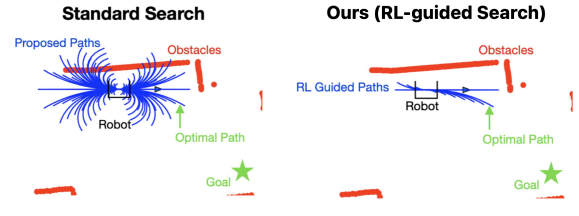


Fig. 1. a) Diagram of our collision avoidance system, and our robotic platform with a self-balancing base with differential drive, an onboard Linux computer, a 2D 360° lidar scanner, an ultrasonic sensor array, and RGB-D cameras. b) Our training and testing environments. c) Illustration of the RL-guided search with learned search heuristics.

II. RELATED WORK

There's a broad literature on the topic of real-world collision-avoidance, and in the following we discuss its related work on *safety in real-world robots*, *learning from expert demonstration*, *sim-to-real learning*, and *learning from collisions*.

Safety in Real-world Robots. AEB is commonly applied in real-world robots, where AEB performs maximum braking when detecting obstacles or emergency situations. Nonetheless, the AEB system could make sub-optimal decisions such as performing maximum braking too late, which can result in a head-on collision. Therefore, it's safer to plan ahead to avoid getting into a situation where an AEB system has to take over [5]; formulating collision avoidance as one of the cost terms in an overall search or trajectory optimization problem [13][30]. With powerful computer, model simplification and heuristics, such approaches have hope for finding collision-free global optimal solutions. Yet, the computation resource on mobile robot is too limited to perform such expensive computation in addition to other essential tasks like perception [16]. Our work considers a realistic setup that we perform efficient collision avoidance using on-device compute to prevent the robot from getting into an unsafe position. Our work also relates to safe reinforcement learning (RL), such as constrained policy optimization (CPO) [1]. While there are no evidence shows that CPO works in the real world systems, our approach is demonstrated to work in real world.

Learning from Human Demonstrations. A popular way to learn to avoid collisions is to learn from human demonstrations, including imitation learning methods [20], [21], [3], [24], [7], [18], and by learning to avoid human disengagement [12]. The first class of methods (imitation

learning) aim to make a robotic agent mimic human behaviors. The second class of methods (learning to avoid human disengagement) aim to make a robotic agent generate actions that avoid human disengagement, which is similar to our approach where we learn to reduce the amount of AEB activation. Although these approaches have demonstrated their effectiveness in collision avoidance, they require a lot of human demonstration data, which is expensive to collect. Our approach on the other hand, learns from AEB activation signals, which require no human demonstrations.

Sim-to-Real Transfer. Another family of collision avoidance involves learning in simulation, and then performing sim-to-real transfer [25], [19], [9], [29], [31]. Although simulation offers us a large amount of training data when compared to the real-world, the enormous sim-to-real domain gap may hinder the learning algorithms to generalize. Our approach learns directly in the real world, and evidence shows that direct real world learning is preferable to applying sim-to-real transfer [15].

Learning from Collisions. Our work also relates to learning collision avoidance by experiencing collisions [14], [6], [11], in which collision is regarded to be a valuable learning signal. However these approaches will inevitably cause physical damage to robotic agents, and the environment in which they operate in. On the other hand, our approach regards AEB activation as a valuable learning signal, which is safer in the real world.

III. METHOD

We present our collision avoidance system in Fig. 1 (a), noting that our method runs in parallel with upstream tasks, such as navigation planning and human control. Our approach takes as input the robot state from odometry, the lidar and ultrasonic scans, maximum braking signals, and the

control commands from the upstream tasks. The output is a corrective control command to the upstream reference tasks, which avoids collision and provides favorable behavior (fast speed, smooth control, etc.). There are two stages within our collision avoidance: *maximum braking and collision avoidance checks* (details in Sec. III-A) and *RL policy and search* (details in Sec. III-B). In the first stage, we determine whether the robot requires maximum braking, or a corrective control command through our learned search. In the second stage, we apply a RL-guided search to output corrective control commands with the goal of 1) reducing the frequency of emergency interventions and 2) avoiding collision efficiently. We introduce important notations in the following.

- Robot states $\mathbf{x} = (x, y, \theta, v, \omega)$ with x/y being 2D euclidean coordinates, θ being the robot's yaw, and v/ω being the robot's linear velocity/angular velocity.
- Reference control commands (v_{ref}, ω_{ref}) are from upstream navigation planning¹ or human control².
- Corrective control commands (v_c, ω_c) are outputted by our collision avoidance module.
- Maximum linear & angular acceleration $(a_{\max}^v, a_{\max}^\omega)$.
- Maximum and minimum linear velocity $(v_{\max}, -v_{\max})$.
- Reaction time t_r is a hyper-parameter, representing our collision avoidance module's latency. We set it as 50 ms.
- Plan-ahead time t_p is a hyper-parameter, representing the time horizon for trajectory planning, according to the maximum braking capability of the robot. t_p is a dynamic parameter (changing with respect to robot velocity), and depends on the collision avoidance module's latency (t_r), current linear velocity (v), and maximum linear acceleration (a_{\max}^v). We set it as $t_p = t_r + v/(2a_{\max}^v)$.
- Robot kinematics $\mathbf{x}_{i+1} := f(\mathbf{x}_i)$ is defined as

$$\mathbf{x}_{i+1} := f(\mathbf{x}_i) = \begin{cases} x_{i+1} &= x_i + v_i \cos(\theta_i) t_r \\ y_{i+1} &= y_i + v_i \sin(\theta_i) t_r \\ \theta_{i+1} &= \theta_i + \omega_i t_r \\ v_{i+1} &= v_c \\ \omega_{i+1} &= \omega_c \end{cases}.$$

- Robot trajectory $\text{traj}(v, \omega, \Delta t)$ is defined as

$$\text{traj}(v, \omega, \Delta t) := [\mathbf{x}_0, \mathbf{x}_1, \mathbf{x}_2, \dots, \mathbf{x}_{\Delta t/t_r}],$$

where t_r is considered to be the time step and Δt is the total time horizon. The initial robot state $\mathbf{x}_0 = (0, 0, 0, v, \omega)$ since we use an ego-centric robot frame.

- 2D Lidar scan $\{l_0, l_1, \dots, l_{359}\}$ collects signals from 360°, representing distance in meters.
- 2D ultrasonic scans $\{u_{-45}, u_0, u_{45}\}$ collects signals from $\{-45^\circ, 0^\circ, 45^\circ\}$, representing distance in meters. We leverage ultrasonics to detect glass surfaces.

¹The upstream navigation policy is generated from the navigation stack (i.e., we use ROS [27] package), which considers a different set of inputs: the front and back rgb-d cameras, and visual odometry.

²Our collision avoidance system also works with human control.

- Obstacles $\mathbb{O}_s \subset \mathbb{R}^2$ are registered using lidar and ultrasonic signals $\{l_0, l_1, \dots, l_{359}, u_{-45}, u_0, u_{45}\}$ within t_r .
- Maximum Braking Status $\sigma = 1$ when maximum braking triggers; otherwise $= 0$.

A. Maximum Braking and Collision Avoidance Check

According to the robot's current state and the surrounding obstacles, we perform a maximum braking and collision avoidance check, and we apply corrective action to the control commands. If the maximum braking check is satisfied, we apply maximum braking to bring the robot to a complete stop. If the maximum braking check is not satisfied, but the collision avoidance is, we search for a corrective control command using our RL-guided search. If neither check is satisfied, our system maintains the upstream control. In the following, we first define collision, then discussing the maximum braking and collision avoidance check.

Collision. We define $\mathbb{E}(\mathbf{x}) \in \mathbb{R}^2$ as the set of points in 2D space by the robot's shape at state \mathbf{x} . A collision occurs between the robot's trajectory $\text{traj}(v, \omega, \Delta t)$ and the set of obstacles $\mathbb{O}_s \subset \mathbb{R}^2$ if:

$$\bigcup_{\mathbf{x} \in \text{traj}(v, \omega, \Delta t)} (\mathbb{E}(\mathbf{x}) \cap \mathbb{O}_s) \neq \emptyset.$$

Maximum Braking Check. We adopt maximum braking control when the robot's trajectory along the plan-ahead time t_p , denoted as $\text{traj}(v, \omega, t_p)$, collides with obstacles, formulated as $\bigcup_{\mathbf{x} \in \text{traj}(v, \omega, t_p)} \mathbb{E}(\mathbf{x}) \cap \mathbb{O}_s \neq \emptyset$.

Collision Avoidance Check. If the maximum braking check is not satisfied, then we expand the plan-ahead time to βt_p ³ to see if the robot collides with obstacles that are further away. It can be formulated as $\bigcup_{\mathbf{x} \in \text{traj}(v, \omega, \beta t_p)} \mathbb{E}(\mathbf{x}) \cap \mathbb{O}_s \neq \emptyset$. If there is a collision, then we perform our RL-guided search for a corrective control command.

B. RL Policy and Search

Our RL-guided search is inspired by the Dynamic Window Approach (DWA) [5]. The DWA approach defines a dynamic window $W = [v_{\text{lower}}, v_{\text{upper}}] \times [\omega_{\text{lower}}, \omega_{\text{upper}}]$ identifying the set formed by the Cartesian product of values in the range between lower and upper linear velocity, and angular velocity values. DWA then searches for a corrective control command $(v_c, \omega_c) \in W$. Alternatively, our approach introduces additional parameters to shrink the dynamic window W via a RL policy, then searching inside of the smaller W . In the following, we define the dynamic window, discuss the RL policy and reward, and lastly discuss the search.

Dynamic Window. In the DWA approach [5], the standard dynamic window W_{standard} is defined using the current robot velocity (v, ω) , the maximum linear and angular acceleration $(a_{\max}^v, a_{\max}^\omega)$, and the robot reaction-time t_r :

$$[v - a_{\max}^v t_r, v + a_{\max}^v t_r] \times [\omega - a_{\max}^\omega t_r, \omega + a_{\max}^\omega t_r].$$

However, searching in W_{standard} can be inefficient since the ranges between the lower and upper velocities can be large. Hence, we propose to reduce the search space and shrink

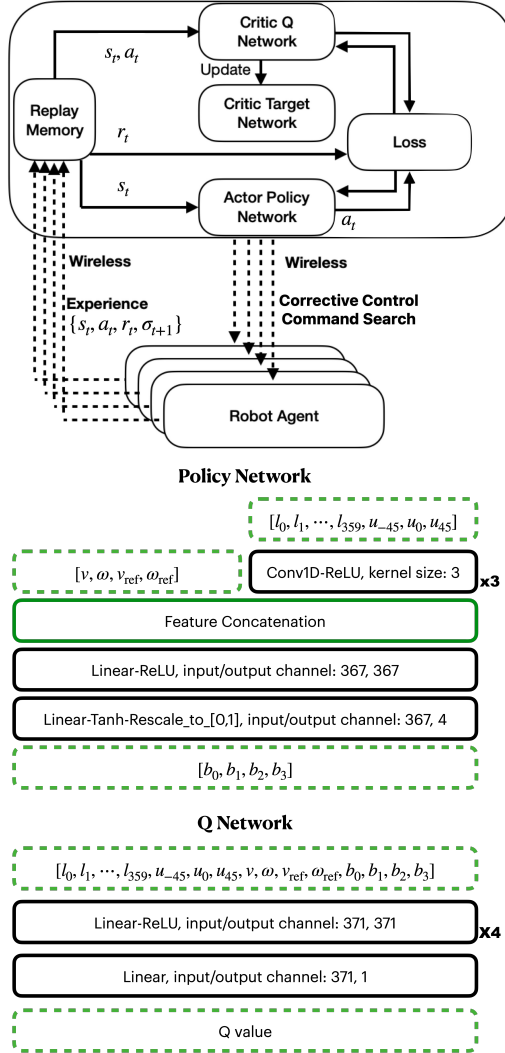
³ $\beta > 1$. As a hyper-parameter, we select $\beta = 2$.

these ranges by introducing four bounded window scales $[b_0, b_1, b_2, b_3] \in [0, 1]^4$ into W_{standard} . The learned window W_{learned} becomes:

$$[v - b_0 a_{\text{max}}^v t_r, v + b_1 a_{\text{max}}^v t_r] \times [\omega - b_2 a_{\text{max}}^\omega t_r, \omega + b_3 a_{\text{max}}^\omega t_r]. \quad (1)$$

Note that $[b_0, b_1, b_2, b_3]$ are the output of our RL policy. We see that the search space of W_{learned} compared to W_{standard} gets reduced by $b_0 b_1 b_2 b_3$.

RL Policy and Reward. We consider a distributed RL training setup with the soft actor critic (SAC) [8] approach. Our robots collect experiences and send them to a central training server, and the training server uses these experiences to train and update the actor's policy network, as well as the critic and critic target networks. The training server sends all robots the updated actor network after a fixed number of training steps. The following figures present the overall setup and network specifications:



For each time step, s_t represents the input to the policy and the critic network, consisting of lidar and ultrasonic scans, robot's linear and angular velocity, and the control commands from the upstream task: $s_t = [l_0, l_1, \dots, l_{359}, u_{-45}, u_0, u_{45}, v, \omega, v_{\text{ref}}, \omega_{\text{ref}}]$.

Procedure 1 Training Algorithm

- 1: Initialize upstream navigation $(v_{\text{ref}}, \omega_{\text{ref}})$
- 2: Initialize experience buffer $\mathcal{D} \leftarrow \emptyset$
- 3: Randomly initialize RL network parameters θ
- 4: RL policy action a_t , observation s_t , reward r_t .
- 5: **for** learning epochs **do**
- 6: $(v_{\text{ref}}, \omega_{\text{ref}}) \leftarrow$ upstream control command
- 7: $s_t \leftarrow \{\text{sensor scans}, v, \omega, v_{\text{ref}}, \omega_{\text{ref}}\}$
- 8: **if** maximum braking check satisfied **then**
- 9: $\sigma_t \leftarrow 1$, perform maximum braking
- 10: $a_t, (v_c, \omega_c) \leftarrow \text{Null}, (-v_{\text{max}}, 0)$
- 11: **else**
- 12: $\sigma_t \leftarrow 0$, do not perform maximum braking
- 13: **if** collision avoidance check satisfied **then**
- 14: $a_t \leftarrow [b_0, b_1, b_2, b_3] \leftarrow$ RL policy network
- 15: $(v_c, \omega_c) \leftarrow$ eq. (4) with $\{s_t, a_t\}$
- 16: **else**
- 17: $a_t, (v_c, \omega_c) \leftarrow \text{Null}, (v_{\text{ref}}, \omega_{\text{ref}})$
- 18: **if** a_{t-1} not Null **then**
- 19: $r_{t-1} \leftarrow$ eq. (2) with $\{s_{t-1}, a_{t-1}, \sigma_t\}$
- 20: $\mathcal{D} \leftarrow \{s_{t-1}, a_{t-1}, r_{t-1}, \sigma_t\}$
- 21: command robot with (v_c, ω_c)
- 22: use \mathcal{D} to update θ using RL

a_t is the output of the policy network and also part of the input to the critic network: $a_t = [b_0, b_1, b_2, b_3]$.

r_t is our reward function. Since we aim to learn corrective control commands that can 1) reduce the number of maximum braking interventions and 2) avoid collision efficiently, we compose r_t to be

$$r_t = -\lambda_1 \sigma_{t+1} - \lambda_2 (b_0 b_1 b_2 b_3) - \lambda_3 J(v_c, \omega_c), \quad (2)$$

where $\lambda_1, \lambda_2, \lambda_3$ are hyper-parameters⁴, σ_{t+1} is the maximum braking status of the next time step, $(b_0 b_1 b_2 b_3)$ represents the size of the search space, and $J(v_c, \omega_c)$ measures the distance between the planned trajectory and the obstacles given control command (v_c, ω_c) . Precisely, we define $J(v_c, \omega_c)$ as

$$J(v_c, \omega_c) = c_1 (v_{\text{max}} - v_c) + c_2 (|v_c - v_{\text{ref}}| + |\omega_c - \omega_{\text{ref}}|) + c_3 \frac{1}{\text{dist}(\mathbb{O}_s, \text{traj}(v_c, \omega_c, \beta t_p))}, \quad (3)$$

where c_1, c_2, c_3 are hyper-parameters⁵, $(v_{\text{max}} - v_c)$ encourages the corrective linear velocity to be fast, $(|v_c - v_{\text{ref}}| + |\omega_c - \omega_{\text{ref}}|)$ minimizes the deviation of corrective control commands from upstream control commands, and $\frac{1}{\text{dist}(\cdot)}$ encourages the robot to stay away from obstacles with $\text{dist}(\mathbb{O}_s, \text{traj})$ distance between the robot's trajectory and the obstacles:

$$\text{dist}(\mathbb{O}_s, \text{traj}) = \min_{\forall (x_s, y_s) \in \mathbb{O}_s, (\hat{x}, \hat{y}) \in \mathbf{x} \in \text{traj}} \|(\hat{x}, \hat{y}) - (x_s, y_s)\|.$$

⁴In our design, $\lambda_1 = 35, \lambda_2 = 10, \lambda_3 = 10$.

⁵In our settings, $c_1 = 0.4, c_2 = 0.2, c_3 = 0.4$

TABLE I
QUANTITATIVE COMPARISONS IN THE TRAINING ENVIRONMENT.

Methods	Search	Learning from AEB	average speed (↑)	collision rate (↓)	time between collision (↑)	goals reached rate (↑)	search size (↓)	unsmoothness (↓)
NoSafety	no	no	0.57 m/s	26.0 %	1.9 min.	70.0 %	n/a	0.26
PureAEB	no	no	0.39 m/s	8.0 %	6.2 min.	82.0 %	n/a	0.41
PureRL	no	yes	0.58 m/s	12.0 %	4.1 min.	72.0 %	n/a	0.61
StandardSearch	yes	no	0.49 m/s	4.0 %	10.5 min.	86.0 %	100.0 %	0.31
Ours	yes	yes	0.68 m/s	2.0 %	23.5 min.	92.0 %	32.0 %	0.17

TABLE II
QUANTITATIVE COMPARISONS IN THE EVALUATION ENVIRONMENT.

Methods	Search	Learning from AEB	average speed (↑)	collision rate (↓)	time between collision (↑)	goals reached rate (↑)	search size (↓)	unsmoothness (↓)
NoSafety	no	no	0.48 m/s	33.3 %	1.5 min.	66.7 %	n/a	0.32
PureAEB	no	no	0.37 m/s	10.0 %	5 min.	76.7 %	n/a	0.44
PureRL	no	yes	0.46 m/s	16.7 %	2.8 min.	70.0 %	n/a	0.64
StandardSearch	yes	no	0.52 m/s	6.7 %	7.2 min.	80.0 %	100.0 %	0.35
Ours	yes	yes	0.66 m/s	3.3 %	13.7 min.	86.7 %	37.0 %	0.19

Search. After we obtain $[b_0, b_1, b_2, b_3]$ from the RL policy network, we perform search for the corrective control command. In particular, we consider a search with granularity of n_v linear and n_ω angular velocity control commands from W_{learned} (eq. (1)) that minimizes $J(v_c, \omega_c)$ (eq. (3)):

$$\begin{aligned}
 (v_c, \omega_c) &= \arg \min_{(v_c, \omega_c)} J(v_c, \omega_c) \\
 \text{s.t. } v_c &\in \{v - b_0 a_{\max}^v t_r, v - b_0 a_{\max}^v t_r + s_v, \dots, v + b_1 a_{\max}^v t_r\} \\
 \omega_c &\in \{\omega - b_2 a_{\max}^\omega t_r, \omega - b_2 a_{\max}^\omega t_r + s_\omega, \dots, \omega + b_3 a_{\max}^\omega t_r\},
 \end{aligned} \tag{4}$$

where $s_v = (b_0 + b_1) a_{\max}^v t_r / n_v$ and $s_\omega = (b_2 + b_3) a_{\max}^\omega t_r / n_\omega$. We note that our learned window W_{learned} provides a more granular search in comparison to W_{standard} , when (n_v, n_ω) are fixed in both cases (we follow this in our work).

IV. EXPERIMENTS

In this section, we perform real-world robot experiments in indoor office environments. Given a goal location, the robots leverage the ROS navigation stack [27] to provide navigation as the upstream task. Our indoor environment contains many different obstacles including glass, humans, office chairs, other robots, etc. We consider 50 random location goals in the training and 30 random goals in the evaluation environments.

Methods of Comparison. We consider four baselines to demonstrate the effectiveness of our method. The first baseline only considers an upstream reference navigation policy, in which the robots have the ability to map, localize, and navigate in a static environment given goal locations, but there is no collision avoidance system. Building upon the first baseline, the second, third, and fourth baselines add a collision avoidance component to correct the reference navigation policy. For the second baseline, its safety system comes from a pure reinforcement learning setting: the reinforcement learning algorithm learns to directly output corrective actions for the robot, when it is triggered by a collision avoidance check according to time horizon βt_p . We use the reward function described in Equation (2), and set the window size

$b_0 b_1 b_2 b_3 = 0$ because no search is performed. For the third baseline, its safety system only utilizes a maximum braking mechanism. The second and third baselines do not perform collision avoidance search, and are triggered when a maximum braking condition is detected. The fourth baseline is the most similar to our approach, but we use the standard dynamic window in [5] (DWA) for performing collision avoidance search. We shorthand the first baseline as NoSafety, the second baseline as PureRL, the third baseline as PureAEB, the fourth baseline as StandardSearch, and our method as Ours. Note that PureRL and Ours both learn with maximum braking signals.

Metrics. We report metrics on maximizing 1) average speed: the mean of the linear speed across all control decisions in (m/s); minimizing 2) collision rate: the ratio of the number of goals resulting in a collision compared to all goals; maximizing 3) time between collision: average number of minutes between collisions; maximizing 4) goals reached rate: the percentage of goals reached out of the total; minimizing 5) search size: the relative search window size compared to that in dynamic window approach [5]; and minimizing 6) unsmoothness: the mean of the linear and lateral accelerations between control decisions. As an example, given two sequential control decisions (v_0, w_0) and (v_1, w_1) , and elapsed time of t we calculate unsmoothness for this step to be $(|v_1 - v_0| + |w_1 - w_0|)/t$. Note that unsmoothness reflects the frequency of maximum braking performed: frequent maximum braking leads to high unsmoothness.

A. Results in Training Environment

We report the results in Table I. First, we compare the methods with and without safety systems. We find that methods with a safety system come with a lower collision rate, larger time between collisions, and a higher goals reached rate (a goal is considered as not reached as soon as a collision occurs). For instance, the collision rate drops from 26.0% to 8.0% from NoSafety to PureAEB, and time between collisions nearly triples. Nonetheless, we also find

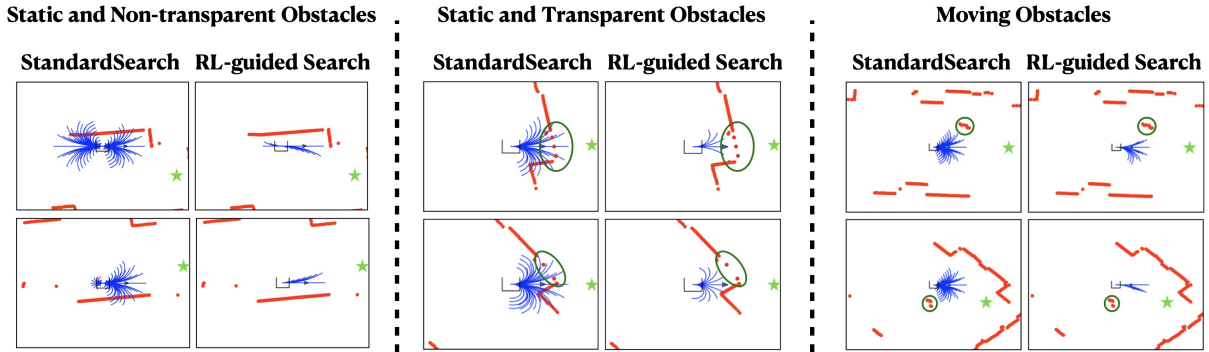


Fig. 2. Qualitative results for obstacle avoidance against different types of obstacles. The goal location is highlighted as a green star. Left: We have obstacles that are static. Middle: We have glass obstacles that are static and transparent (circled in green). Note that the sparse points in the circle are ultrasonic sensory input. Right: We have human obstacles that are dynamic (circled in green). Our approach is able to plan a path away from the human, while still attempting to make progress toward the goal.

that the methods with a safety system (except our approach *Ours*) have lower average speed and higher unsmoothness. We find that there may be compromise between safety (i.e., collision rate) and user experience (i.e., average speed and unsmoothness) when adding safety systems into the robot.

Next, we focus on evaluating the effects of performing collision avoidance search in the safety system. We find that methods that have collision avoidance search can reduce collision rate, increase time between collisions, improve goals reached rate, and reduce unsmoothness. For instance, the collision rate drops from 8.0% to 4.0%, the goals reached rate increases from 82.0% to 86.0%, and the unsmoothness drops from 0.41 to 0.31 from PureAEB to StandardSearch. Nonetheless, the average speed can be a compromise of adding search: we observe a reduction of average speed from 0.58 m/s to 0.49 m/s from PureRL to StandardSearch. A possible explanation is that search introduces turns and speed reduction for the robots.

Third, we compare StandardSearch and *Ours*, which *Ours* additionally leverages maximum braking signals to 1) reduce the frequency of maximum braking and 2) search more efficiently. We observe that all metrics improved significantly from StandardSearch to *Ours*, which suggests that maximum braking provides a good signal for collision avoidance learning.

Comparisons in the Evaluation Environment. Now, we evaluate the generalization capability of our method in the evaluation environment in Table II. Note that the experiments are performed post-training (we do not re-train the networks in the evaluation environment) and the training and the evaluation environments contain different layout and obstacles. When compared to the training environment, the overall trend is similar in the evaluation environment: our approach *Ours* achieves the best performance on all metrics.

Conclusion. Our experiments suggest that maximum braking can serve as a good learning signal for the robotic agent to learn to avoid collision. Nonetheless, learning to avoid maximum braking in a pure RL setting was not sufficient to provide safety (the PureRL approach). Alternatively, our method *Ours* leverages maximum braking signals to improve trajectory search, which provided better search efficiency, quality, and lower collision rates.

B. Qualitative Results

In this section, we provide qualitative results for our method against obstacles that are static and non-transparent (walls and furniture), static and transparent (glass), and moving (human). The comparisons are made between methods with safety system and with search in the safety system: StandardSearch and *Ours*.

Static, Non-transparent Obstacles. We present the results in the left figure of Fig. 2. First, we find our approach (*Ours*) explores far fewer trajectories in a much more confined search window. Next we observe that the bounded search space contains little to no trajectories that cause collision, and includes trajectories that take the robot closer to the goal. The results provide insight into how our method improves the efficiency of search by leveraging maximum braking signals.

Static, Transparent Obstacles (glass). We present the results in the middle figure of Fig. 2. Note that in this setup, the goal location is on the other side of a glass surface. When compared to the traditional search (StandardSearch), we find our method (*Ours*) effectively learns to leverage sparse ultrasonic sensory input to avoid glass surfaces.

Moving Obstacles (Human). We present the results in the right figure of Fig. 2. We find our approach (*Ours*) can also avoid collisions with humans. Note that our system does not treat moving obstacles differently than static obstacles, and hence having a low latency between control cycles for collision avoidance is important. The result suggests that *Ours* can perform an efficient collision avoidance, and for future work we plan to explore more complex methods for obstacle avoidance against dynamic objects.

V. CONCLUSION

In this work, we leverage the activation of emergency interventions as a learning signal for a real-world reinforcement learning guided search method that 1) reduces the frequency of triggering emergency interventions and 2) reduces the search space with learned search heuristics. Our approach enables direct and safe real-world learning without human intervention or overtake. In our real-world experiments, we show our method outperforms other collision avoidance baselines. For future work, we plan to extend our setting to non-stationary multi-agent environments with potentially diverse dynamic obstacles.

REFERENCES

- [1] Joshua Achiam, David Held, Aviv Tamar, and Pieter Abbeel. Constrained policy optimization. In *International conference on machine learning*, pages 22–31. PMLR, 2017.
- [2] Chao Cao, Peter Trautman, and Soshi Iba. Dynamic channel: A planning framework for crowd navigation. In *2019 International Conference on Robotics and Automation (ICRA)*, pages 5551–5557, 2019.
- [3] Felipe Codevilla, Matthias Müller, Antonio López, Vladlen Koltun, and Alexey Dosovitskiy. End-to-end driving via conditional imitation learning. In *2018 IEEE international conference on robotics and automation (ICRA)*, pages 4693–4700. IEEE, 2018.
- [4] Wei Ding, Madan Ravi Ganesh, Robert N. Seuringhaus, Jason J. Corso, and Dimitra Panagou. Real-time model predictive control for keeping a quadrotor visible on the camera field-of-view of a ground robot. In *2016 American Control Conference (ACC)*, pages 2259–2264, 2016.
- [5] Dieter Fox, Wolfram Burgard, and Sebastian Thrun. The dynamic window approach to collision avoidance. *IEEE Robotics & Automation Magazine*, 4(1):23–33, 1997.
- [6] Dhiraj Gandhi, Llerel Pinto, and Abhinav Gupta. Learning to fly by crashing. In *2017 IEEE/RSJ International Conference on Intelligent Robots and Systems (IROS)*, pages 3948–3955. IEEE, 2017.
- [7] Alessandro Giusti, Jérôme Guzzi, Dan C Cireşan, Fang-Lin He, Juan P Rodríguez, Flavio Fontana, Matthias Faessler, Christian Forster, Jürgen Schmidhuber, Gianni Di Caro, et al. A machine learning approach to visual perception of forest trails for mobile robots. *IEEE Robotics and Automation Letters*, 1(2):661–667, 2015.
- [8] Tuomas Haarnoja, Aurick Zhou, Pieter Abbeel, and Sergey Levine. Soft actor-critic: Off-policy maximum entropy deep reinforcement learning with a stochastic actor. In *International conference on machine learning*, pages 1861–1870. PMLR, 2018.
- [9] Noriaki Hirose, Fei Xia, Roberto Martín-Martín, Amir Sadeghian, and Silvio Savarese. Deep visual mpc-policy learning for navigation. *IEEE Robotics and Automation Letters*, 4(4):3184–3191, 2019.
- [10] Wesley Hulshof, Iain Knight, Alix Edwards, Matthew Avery, and Colin Grover. Autonomous emergency braking test results. In *Proceedings of the 23rd International Technical Conference on the Enhanced Safety of Vehicles (ESV)*, pages 1–13. National Highway Traffic Safety Administration Washington, DC, 2013.
- [11] Gregory Kahn, Pieter Abbeel, and Sergey Levine. Badgr: An autonomous self-supervised learning-based navigation system. *IEEE Robotics and Automation Letters*, 6(2):1312–1319, 2021.
- [12] Gregory Kahn, Pieter Abbeel, and Sergey Levine. Land: Learning to navigate from disengagements. *IEEE Robotics and Automation Letters*, 6(2):1872–1879, 2021.
- [13] Gregory Kahn, Adam Villafior, Bosen Ding, Pieter Abbeel, and Sergey Levine. Self-supervised deep reinforcement learning with generalized computation graphs for robot navigation. In *2018 IEEE International Conference on Robotics and Automation (ICRA)*, pages 5129–5136. IEEE, 2018.
- [14] Gregory Kahn, Adam Villafior, Vitchyr Pong, Pieter Abbeel, and Sergey Levine. Uncertainty-aware reinforcement learning for collision avoidance. *arXiv preprint arXiv:1702.01182*, 2017.
- [15] Robert Kirk, Amy Zhang, Edward Grefenstette, and Tim Rocktäschel. A survey of generalisation in deep reinforcement learning. *arXiv preprint arXiv:2111.09794*, 2021.
- [16] Steven M LaValle. Planning algorithms, 2006.
- [17] Maxim Likhachev and Sven Koenig. Lifelong planning for mobile robots. In *Advances in Plan-Based Control of Robotic Agents*, pages 140–156. Springer, 2002.
- [18] Antonio Loquercio, Ana I Maqueda, Carlos R Del-Blanco, and Davide Scaramuzza. Dronet: Learning to fly by driving. *IEEE Robotics and Automation Letters*, 3(2):1088–1095, 2018.
- [19] Matthias Müller, Alexey Dosovitskiy, Bernard Ghanem, and Vladlen Koltun. Driving policy transfer via modularity and abstraction. *arXiv preprint arXiv:1804.09364*, 2018.
- [20] Urs Muller, Jan Ben, Eric Cosatto, Beat Flepp, and Yann Cun. Off-road obstacle avoidance through end-to-end learning. *Advances in neural information processing systems*, 18, 2005.
- [21] Yunpeng Pan, Ching-An Cheng, Kamil Saigol, Keuntaek Lee, Xinyan Yan, Evangelos Theodorou, and Byron Boots. Agile autonomous driving using end-to-end deep imitation learning. *arXiv preprint arXiv:1709.07174*, 2017.
- [22] Erik Rosen. Autonomous emergency braking for vulnerable road users. In *IRCOBI conference*, volume 2013, pages 618–627, 2013.
- [23] Christoph Rösmann, Frank Hoffmann, and Torsten Bertram. Integrated online trajectory planning and optimization in distinctive topologies. *Robotics and Autonomous Systems*, 88:142–153, 2017.
- [24] Stéphane Ross, Narek Melik-Barkhudarov, Kumar Shaurya Shankar, Andreas Wendel, Debadepta Dey, J Andrew Bagnell, and Martial Hebert. Learning monocular reactive uav control in cluttered natural environments. In *2013 IEEE international conference on robotics and automation*, pages 1765–1772. IEEE, 2013.
- [25] Fereshteh Sadeghi and Sergey Levine. Cad2rl: Real single-image flight without a single real image. *arXiv preprint arXiv:1611.04201*, 2016.
- [26] Brual C Shah, Petr Švec, Ivan R Bertaska, Armando J Sinisterra, Wilhelm Klingner, Karl von Ellenrieder, Manhar Dhanak, and Satyandra K Gupta. Resolution-adaptive risk-aware trajectory planning for surface vehicles operating in congested civilian traffic. *Autonomous Robots*, 40(7):1139–1163, 2016.
- [27] Stanford Artificial Intelligence Laboratory et al. Robotic operating system.
- [28] Petr Švec, Atul Thakur, Eric Raboin, Brual C Shah, and Satyandra K Gupta. Target following with motion prediction for unmanned surface vehicle operating in cluttered environments. *Autonomous Robots*, 36(4):383–405, 2014.
- [29] Patrick Wenzel, Torsten Schön, Laura Leal-Taixé, and Daniel Cremers. Vision-based mobile robotics obstacle avoidance with deep reinforcement learning. In *2021 IEEE International Conference on Robotics and Automation (ICRA)*, pages 14360–14366. IEEE, 2021.
- [30] Xiaojing Zhang, Alexander Liniger, and Francesco Borrelli. Optimization-based collision avoidance. *IEEE Transactions on Control Systems Technology*, 29(3):972–983, 2021.
- [31] Wenshuai Zhao, Jorge Peña Queralta, and Tomi Westerlund. Sim-to-real transfer in deep reinforcement learning for robotics: a survey. In *2020 IEEE Symposium Series on Computational Intelligence (SSCI)*, pages 737–744. IEEE, 2020.